Journal of Materials Chemistry A

Accepted Manuscript

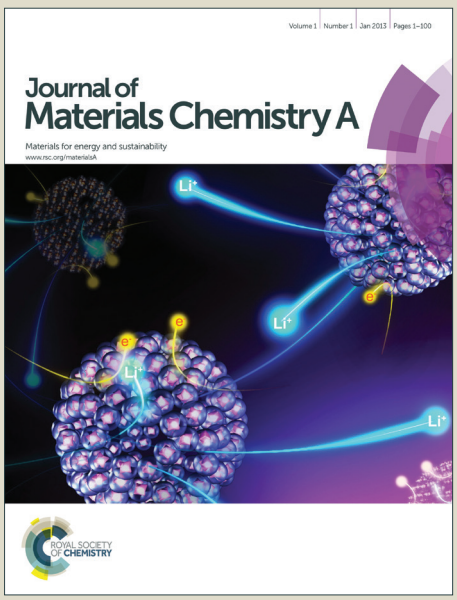

ROYAL SOCIETY OF CHEMISTRY

www.rsc.org/materialsA

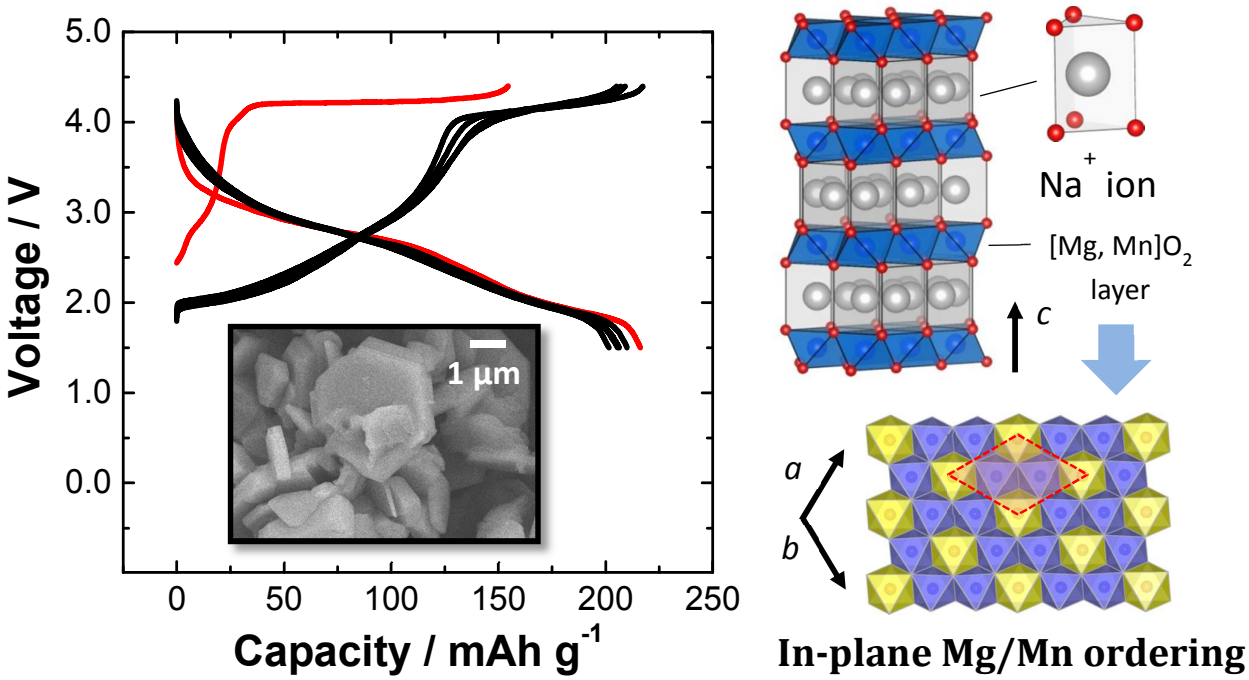

New high-capacity electrode materials made from only the Earth-abundant elements

Cite this: DOI: 10.1039/c0xx00000x

www.rsc.org/xxxxxx

ARTICLE TYPE

New electrode material for rechargeable sodium batteries: P2-type $Na_{2/3}[Mg_{0.28}Mn_{0.72}]O_2$ with anomalously high reversible capacity

Naoaki Yabuuchi,[a,b] Ryo Hara,[a] Kei Kubota,[a,b] Jens Paulsen,[c] Shinichi Kumakura[d] and Shinichi Komaba*[a,b]

Received (in XXX, XXX) Xth XXXXXXXXX 20XX, Accepted Xth XXXXXXXXX 20XX
DOI: 10.1039/b000000x

P2-type $Na_{2/3}[Mg_{0.28}Mn_{0.72}]O_2$ is prepared and electrode performance in Na cells is first provided. The sample surprisingly delivers large reversible capacity (220 mAh g^{-1}) even though electrochemically inactive magnesium ions are enriched in the host structure. This new electrode material is potentially utilized for rechargeable batteries made from only Earth-abundant elements.

Recently, the research interest for the large-scale batteries is rapidly increasing to realize the electrical energy storage (EES).[1] This movement has renewed the research interest for sodium ions as charge carriers for the energy storage technology based on electrochemical reaction because the demand and price of lithium, which is classified as a minor metal and a less abundant element, are continuously increasing after the commercialization of lithium-ion batteries.[2] Our group has demonstrated that lithium-free rechargeable batteries, that is Na-ion batteries (NIB), consisting of hard-carbon and nickel/manganese layered oxides as negative and positive electrodes, respectively, can store/deliver the electricity with moderate energy density.[3] To realize the EES system with advanced NIBs, the material abundance of the Earth's crust is of primary importance to design the positive electrode materials with high capacity. Manganese oxides classified as P2-type layered materials are the potential candidate as high-capacity and cost-effective electrode materials.[4, 5] Although P2-Na_xMnO_2 delivers large reversible capacity, operating voltage based on a redox couple of Mn^{3+}/Mn^{4+} is relatively low as positive electrode materials. Recently, we have reported that partial substitution of iron for manganese is an effective method to increase the operating voltage based on a redox couple of Fe^{3+}/Fe^{4+}.[6] Alternative approach is to use a redox reaction of oxide ions, similar to lithium-excess manganese oxides, $Li[Li_{1/3}Mn_{2/3}]O_2$ (Li_2MnO_3), and its solid solutions known as high-capacity electrode materials in Li cells,[7-10] and very recently, we have demonstrated that P2-type $Na_{5/6}[Li_{1/4}Mn_{3/4}]O_2$ is the promising candidate as high-energy manganese-based positive electrode materials.[11] Although the necessity of lithium to activate the redox reaction of oxide ions (and this process often results in partial oxygen loss from the crystal lattice) and to increase the energy density could limit its use for the application of EES, this concept, the use of the redox reaction of oxide ions, could not be limited by lithium and could be extended to other elements. Herein, we first report that magnesium, which is the Earth-abundant element, is also the effective element to activate the redox reaction of oxide ions for P2-type manganese-based electrode materials, similar to the excess lithium in $Li[Li_{1/3}Mn_{2/3}]O_2$. The magnesium-substituted manganese oxides show surprisingly large reversible capacity in Na cells (and not in Li cells) even though it had been thought that the increase in the substitution amount of magnesium as the redox "inactive" element inevitably results in the loss of reversible capacity based on the Mn^{3+}/Mn^{4+} redox. In this article, we describe synthesis, crystal structures, and anomalous electrochemical properties of P2-type $Na_{2/3}[Mg_{0.28}Mn_{0.72}]O_2$ as the promising positive electrode material made from only the Earth-abundant elements.

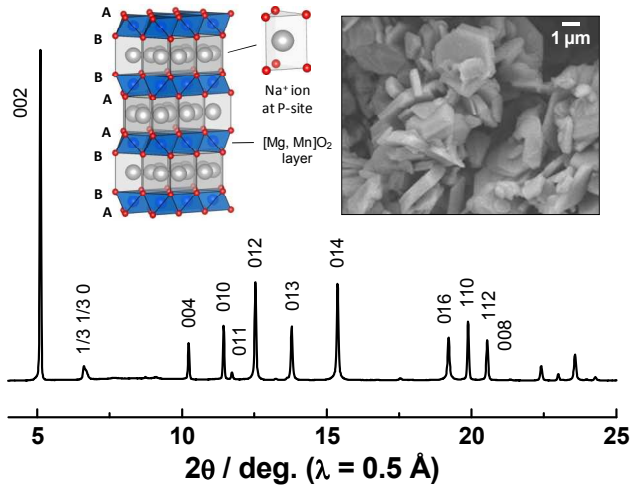

Figure 1. The SXRD pattern of P2-type $Na_{2/3}[Mg_{0.28}Mn_{0.72}]O_2$. A schematic illustration of the P2-type layered structure drawn using the program VESTA[12] and a SEM image of the sample are also shown.

[a] *Department of Applied Chemistry, Tokyo University of Science, 1-3 Kagurazaka, Shinjuku, Tokyo 162-8601, Japan. E-mail: komaba@rs.kagu.tus.ac.jp*
[b] *Elements Strategy Initiative for Catalysts and Batteries (ESICB), Kyoto University, Katsura, Kyoto, 615-8520, Japan*
[c] *Umicore Korea Limited, 401, Chaam-dong, Cheonan-city, Chungnam, 330-200, Korea*
[d] *Umicore Japan KK, Kobe Plant, 4-2-8 Minami-machi, Minatojima, Chuo-ku, Kobe, 650-0047, Japan*

† Electronic Supplementary Information (ESI) available: the result of Rietveld analysis, electrode performance of $Na_{2/3}[Mg_{0.28}Mn_{0.72}]O_2$ with different cut-off voltage, Na^+/Li^+ ion-exchange of $Na_{2/3}[Mg_{0.28}Mn_{0.72}]O_2$ and electrode performance of the ion-exchanged product, EDX spectra after the electrochemical cycle, SXRD patterns of electrochemically charged samples and the change in lattice parameters.. See DOI: 10.1039/b000000x/

Table 1. Crystallographic parameters refined by the Rietveld method on the synchrotron X-ray diffraction pattern of P2-type $Na_{2/3}[Mg_{0.28}Mn_{0.72}]O_2$.

$P2\text{-}Na_{2/3}[Mg_{0.28}Mn_{0.72}]O_2$						
S.G. $P6_3/mmc$; a = 2.8972(2) Å, c = 11.213(1) Å						
R_{wp} = 8.27%, R_B = 3.86%, R_F = 2.61%, S = 1.04						
atom	site	g	x	y	z	B (Å²)
Na_f	2b	0.276(3)	0	0	1/4	4.8(2)
Na_e	2d	0.391(3)	1/3	2/3	3/4	3.9(2)
Mg	2a	0.28	0	0	0	0.35(2)
Mn	2a	0.72	0	0	0	0.35(2)
O	4f	1.0	1/3	2/3	0.0875(2)	0.88(5)

$Na_{2/3}[Mg_{0.28}Mn_{0.72}]O_2$ was prepared by solid-state reaction of Na_2CO_3 (Kanto Chem. Co., Ltd., purity: 99.5%), $(MgCO_3)_4Mg(OH)_2{\bullet}5H_2O$ (Kanto Chem. Co., Ltd., purity: 42.8% as MgO), and $MnCO_3$ (Kishida Chem. Co., Ltd., 44% as the Mn content), according to the preparation method of P2-type $Na_{2/3}[Mg_xMn_{1-x}]O_2$ ($1/5 \leq x \leq 1/3$) reported in the literature.[13] These starting materials were mixed using a mortar and pestle, and then pressed into a pellet. The pellet was heated at 900 °C for 12 h in air. The pellet was taken out from the heated furnace without a cooling process, and then immediately transferred into an argon-filled glove box. The pellet was cooled to room temperature in the glove box and was kept inside it to avoid the contact with moisture in air.

Crystal structures of $Na_{2/3}[Mg_{0.28}Mn_{0.72}]O_2$ were examined by synchrotron X-ray diffraction at the beam line BL02B2, SPring-8 in Japan, equipped with a large Debye-Scherrer camera.[14] To minimize the effect of X-ray absorption by samples, a wavelength of incident X-ray beam was set to 0.5 Å using a silicon monochromator, which was calibrated with a CeO_2 standard. **Figure 1** shows a synchrotron X-ray diffraction (SXRD) pattern of $Na_{2/3}[Mg_{0.28}Mn_{0.72}]O_2$. All diffraction lines can be indexed into a hexagonal lattice with a space group symmetry of $P6_3/mmc$, except the diffraction line at 6.6 degrees (d = 4.3 Å) and some weak diffraction lines from impurity phases. The impurity phases were assigned into Na_2MnO_4, $MgMn_2O_4$ etc. The diffraction line at 6.6 degrees can be assigned to "1/3 1/3 0" superlattice line, suggesting the formation of $\sqrt{3}a \times \sqrt{3}a$-type in-plane ordering between (Mg^{2+}, Mn^{3+}) and Mn^{4+}, and the result is consistent with the literature.[13] However, another supperlattice line "1/3 1/3 2" was not observed at 8.3 degrees. The results imply that the presence of stacking faults of the superlattice layers along c-axis direction, as discussed in our previous article for the Na-Li-Mn system.[11] Therefore, Rietveld analysis was conducted on the SXRD pattern of $Na_{2/3}[Mg_{0.28}Mn_{0.72}]O_2$, except the region, in which the superlattice lines are observed (6.0 – 9.5 degrees, corresponding to the 3.0 – 4.8 Å of d-values). The program of RIETAN-FP was used for the Rietveld analysis.[15] Refined structural parameters are summarized in Table 1, and the refined result is also shown in Supporting Figure S1. The result of the Rietveld analysis indicates that $Na_{2/3}[Mg_{0.28}Mn_{0.72}]O_2$ crystallizes into a P2-type layered structure, in which sodium ions are accommodated between MeO_2 slabs (AB and BA layers in Figure 1) consisting of edge-sharing (Mn, Mg)O_6 octahedra. Large B-values (3.9 – 4.8 Å^2) are observed at prismatic sodium sites and such phenomenon is often observed in the P2-type phase with vacant sodium sites, which could be indicative of fast self-diffusion of Na ions in the framework structure.[11] The cation ordering between Mn and Mg ions and specific sites for Na ions were not taken into account in this model, and the crystallographic parameters summarized in Table 1 were obtained as the averaged structure.

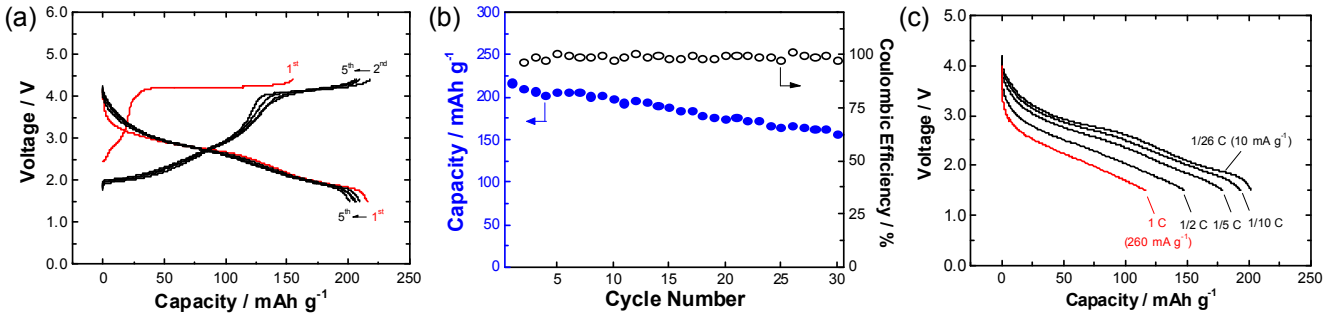

Figure 2. Electrochemical characterization of $Na_{2/3}[Mg_{0.28}Mn_{0.72}]O_2$ in Na cells; (a) charge/discharge curves of the Na/$Na_{2/3}[Mg_{0.28}Mn_{0.72}]O_2$ cell cycled at a rate of 10 mA g^{-1} in voltage ranges of 1.5 – 4.4 V. Discharge capacity and Coulombic efficiency of the cell are plotted in (b). (c) Rate-capability of the Na/ $Na_{2/3}[Mg_{0.28}Mn_{0.72}]O_2$ cell. The cell was charged at a rate of 10 mA g^{-1} to 4.4 V, and then discharged to 1.5 V at different current density. Sample loading of the electrodes used is (a, b) 2.2 and (c) 3.2 mg cm^{-2}.

Particle morphology of $Na_{2/3}[Mg_{0.28}Mn_{0.72}]O_2$, observed by using a scanning electron microscope (JSM-7001F/SHL, JEOL Co., Ltd.) operated at 10 keV of acceleration voltage. Particle morphology of $Na_{2/3}[Mg_{0.28}Mn_{0.72}]O_2$ (**Figure 1)** is found to be well-crystallized hexagonal plate shape with 1 – 3 μm in diameter and 0.3 - 1 μm in thickness even though non-uniform distribution for particle size is noted.

Electrode performance of the well-characterized $Na_{2/3}[Mg_{0.28}Mn_{0.72}]O_2$ sample was further examined in Na cells. Detailed setup of the electrochemical characterization was described in the **Supplementary Information**. Since the majority (85%) of manganese ions exists as a tetravalent state, $Na_{2/3}[Mg_{0.28}Mn_{0.72}]O_2$ had been expected to be electrochemically less active compared to P2-type $Na_{2/3}[Mn^{3+}{}_{2/3}Mn^{4+}{}_{1/3}]O_2$. Indeed, it has been reported that reversible capacity for P2-$Na_{2/3}[Mn_{1-x}Mg_x]O_2$ ($0 \leq x \leq 0.2$) in the voltage range of 1.5 and 4.0 V decreases as increase in the substitution amount of magnesium for manganese ions.[16] However, P2-type $Na_{2/3}[Mg_{0.28}Mn_{0.72}]O_2$

is surprisingly electrochemically active and delivers >200 mAh g^{-1} of reversible capacity in the Na cell as shown in **Figure 2**. A well-defined voltage plateau is observed at 4.2 V vs. Na in the initial charge process, and large discharge capacity is observed after charge beyond the voltage plateau. Note that such large capacity is only observed after charge to high voltage as shown in **Supporting Figure S2**. Such the voltage plateau at 4.2 V is still observed for the 2nd cycle. Relatively large reversible capacity of >150 mAh g^{-1} is observed after 30 cycles (**Figure 2b**). Additionally, the sample shows acceptable rate-capability as the electrode materials as shown in **Figure 2c**. Over 50% of capacity is retained even at 1 C rate (260 mA g^{-1}) using the micrometer-sized and dense particles. Nanosized particles are not required to obtain large reversible capacity in Na cells.

The appearance of the voltage plateau (at ca. 4.2 V vs. Na and 4.5 V vs. Li) in **Figure 2a** reminds us the characters of Li_2MnO_3-based electrode materials in Li cells.[7-9] From the electrochemical behavior of P2-$Na_{2/3}[Mg_{0.28}Mn_{0.72}]O_2$ in the Na cells, the oxide ions seem to contribute the redox process in P2-$Na_{2/3}[Mg_{0.28}Mn_{0.72}]O_2$, and this result is the first evidence that Mg in transition metal layers is also used to activate the oxide ion redox, similar to Li in $Li[Li_{1/3}Mn_{2/3}]O_2$ and its solid solutions. It is believed that this chemistry is uniquely observed in the Na system, not in the Li. Indeed, the oxidation of oxide ions is thought to be difficult in a Li counterpart with Mg (See the **Supporting Figure S3** for more details).

To further study the reaction mechanisms of P2-type $Na_{2/3}[Mg_{0.28}Mn_{0.72}]O_2$, the structural changes on electrochemical cycles in Na cells were examined by ex-situ SXRD. **Figure 3** shows the SXRD patterns of electrochemically cycled P2-$Na_x[Mg_{0.28}Mn_{0.72}]O_2$ in the Na cells. Oxide ions are partly oxidized in the $Li[Li_{1/3}Mn_{2/3}]O_2$-based electrode materials with the appearance of the voltage plateau, and the oxidation of oxide ions partly results in the release of oxygen as molecules (and also as CO/CO_2), resulting in the in-plane cation rearrangements in the framework structure. Generally, the evidence of in-plane cation ordering is lost after oxygen loss and cation rearrangements. Superlattice lines disappear after charge beyond the voltage plateau in the $Li[Li_{1/3}Mn_{2/3}]O_2$ system.[8, 17, 18] Our group recently confirmed similar processes in the P2-$Na_{5/6}[Li_{1/4}Mn_{3/4}]O_2$.[11] It is noted that the superlattice lines for $Na_x[Mg_{0.28}Mn_{0.72}]O_2$ are still visible after full charge to 4.4 V. For both P2-$Na_x[Li_{1/4}Mn_{3/4}]O_2$ and P2-$Na_x[Mg_{0.28}Mn_{0.72}]O_2$, large reversible capacity of 200 mAh g^{-1} is similarly observed, the in-plane structural reorganization process is clearly different. In-plane cation ordering should be retained in $Na_x[Mg_{0.28}Mn_{0.72}]O_2$ because superlattice lines are still observed even after the 5th cycle (**Figure 3**). Chemical analysis by SEM/EDX suggests that magnesium ions still exist in the sample as shown in **Supporting Figure S4**. This result suggests that magnesium ions are not extracted from P2-$Na_x[Mg_{0.28}Mn_{0.72}]O_2$ by electrochemical reaction. In contrast, Li extraction from transition metal layers in the $Li[Li_{1/3}Mn_{2/3}]O_2$-based electrode materials is generally observed.[8, 17, 18] A question remains here that the oxygen loss from the crystal lattice is also suppressed or not, similar to magnesium ions: A study on detailed charge compensation mechanisms, potentially contributed by the solid-state redox of oxide ions is currently underway in our group, which will be reported elsewhere.

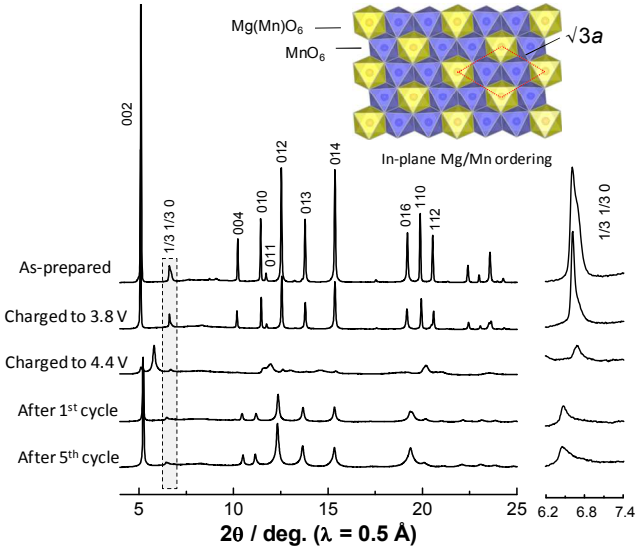

Figure 3. Structural changes of $Na_x[Mg_{0.28}Mn_{0.72}]O_2$ in the Na cells examined by synchrotron X-ray diffractions (SXRD). Highlighted SXRD patterns (marked by a dotted square) are also shown in the inset. Mg and Mn superlattice ordering is still visible after electrochemical cycle tests. Changes in lattice parameters calculated from the SXRD patterns are shown in **Supporting Figure S7**.

Significant peak broadening of diffraction lines is observed after charge (oxidation in Na cells) to 4.4 V in the Na cell. Two phases are found to coexist; O2-type and P2-type layered phases as major and minor phases, respectively (**Supporting Figure S5**). Since large prismatic sites are stabilized by the presence of sodium ions, Na extraction induces glide of MeO_2 slabs, resulting in the formation of an O2-type layered phase.[19] However, the presence of two possible glide vectors for the P2-O2 phase transition often induces stacking faults, and thus broadening of profiles for diffraction lines.[11, 13, 19] Drastic shrinkage of the interlayer distance is normally unavoidable for the P2-O2 phase transition. A change of unit cell volume reaches approximately 15%. This fact could result in the capacity degradation on continuous cycles as shown in **Figure 2b**. Although the large volume change is observed, the P2-O2 phase transition seems to be the reversible process. Major diffraction lines can be assigned into the P2 phase after discharge to 1.5 V (**Supporting Figure S6**). The diffraction line profile becomes broad during cycles compared with those of the as-prepared sample. This change suggests that a small fraction of O2-domains could partly remain in the P2-phase as the staking fault. Changes in the lattice parameters on the electrochemical cycles are summarized in **Supporting Figure S7**. The value of *a*-axis (corresponds to in-plane metal-metal distances) increases from 2.90 Å for the as-prepared sample to 2.96 Å after full discharge (reduction in Na cells). Note that, for P2-Na_xMnO_2 and other P2-type layered oxides with Mn^{3+}/Mn^{4+} redox, in-plane MeO_2 distortion with an orthorhombic lattice is generally observed because of the presence of high-spin Mn^{3+} as Jahn-Teller ions.[20] However, in-plane distortion for $Na_x[Mg_{0.28}Mn_{0.72}]O_2$ was not evidenced as shown in **Figure 3** and **Supporting Figure S6**. This observation suggests that the amount of Mn^{3+} in the sample is relatively low even in the fully discharged state. When the oxygen loss from the crystal lattice occurs on initial charge, Mn^{3+} in the crystal

lattice is enriched after discharge to 1.5 V. Therefore, this fact could also support that the redox reaction of oxide ions is effectively used in $Na_x[Mg_{0.28}Mn_{0.72}]O_2$.

Conclusions

P2-type $Na_{2/3}[Mg_{0.28}Mn_{0.72}]O_2$ is prepared and its electrode performance in Na cells is first reported. P2-type $Na_{2/3}[Mg_{0.28}Mn_{0.72}]O_2$ can deliver anomalously large reversible capacity of >200 mAh g^{-1} in Na cells beyond the theoretical limit of the solid-state redox reaction based on Mn^{3+}/Mn^{4+} couple. Large reversible capacity is expected to originate from the contribution of oxide ions (potentially reversible solid-state reaction of oxide ions and/or partial loss of oxygen, similar to $Li[Li_{1/3}Mn_{2/3}]O_2$-based electrode materials) whereas the Na^+/Li^+ ion-exchanged sample is electrochemically almost inactive in Li cells. The deficiency of sodium ions is a disadvantage of P2-type $Na_{2/3}[Mg_{0.28}Mn_{0.72}]O_2$ (the first discharge capacity is much larger than that of the first charge capacity as shown in **Figure 2a**) when it is intended to design practical NIBs combined with conventional negative electrodes, such as hard-carbon[3] which have no sodium ions to compensate. The compensation for the deficient sodium ions is, therefore, needed to design the NIBs to use full capacity of $Na_{2/3}[Mg_{0.28}Mn_{0.72}]O_2$. One idea to compensate the sodium ions is the addition of sacrificial salts as recently proposed in the literature.[21] P2-type $Na_{2/3}[Mg_{0.28}Mn_{0.72}]O_2$, which is made from only the Earth-abundant elements, is the promising candidate as positive electrode materials for the NIBs.

Acknowledgements

This study was in part granted by The Japan Society for the Promotion of Science through the "Funding for NEXT Program," and MEXT program "Elements Strategy Initiative to Form Core Research Center" (since 2012), MEXT; Ministry of Education Culture, Sports, Science and Technology, Japan. The SXRD experiments were made possible through the support of MEXT (Proposal No. 2013A1681 and 2013B1752), with the approval of the Japan Synchrotron Radiation Research Institute. N.Y. gratefully acknowledges the support of Grant-in-Aid for Young Scientists (B) (No. 24750186) from MEXT.

Notes and references

1. B. Dunn, H. Kamath and J.-M. Tarascon, *Science*, 2011, 334, 928-935.
2. M. D. Slater, D. Kim, E. Lee and C. S. Johnson, *Advanced Functional Materials*, 2013, 23, 947-958.
3. S. Komaba, W. Murata, T. Ishikawa, N. Yabuuchi, T. Ozeki, T. Nakayama, A. Ogata, K. Gotoh and K. Fujiwara, *Advanced Functional Materials*, 2011, 21, 3859-3867.
4. A. Caballero, L. Hernan, J. Morales, L. Sanchez, J. Santos Pena and M. A. G. Aranda, *Journal of Materials Chemistry*, 2002, 12, 1142-1147.
5. A. Mendiboure, C. Delmas and P. Hagenmuller, *Journal of Solid State Chemistry*, 1985, 57, 323-331.
6. N. Yabuuchi, M. Kajiyama, J. Iwatate, H. Nishikawa, S. Hitomi, R. Okuyama, R. Usui, Y. Yamada and S. Komaba, *Nature Materials*, 2012, 11, 512-517.
7. T. Ohzuku, M. Nagayama, K. Tsuji and K. Ariyoshi, *Journal of Materials Chemistry*, 2011, 21, 10179-10188.
8. M. Sathiya, K. Ramesha, G. Rousse, D. Foix, D. Gonbeau, A. S. Prakash, M. L. Doublet, K. Hemalatha and J. M. Tarascon, *Chemistry of Materials*, 2013, 25, 1121-1131.
9. H. Koga, L. Croguennec, M. Ménétrier, K. Douhil, S. Belin, L. Bourgeois, E. Suard, F. Weill and C. Delmas, *Journal of The Electrochemical Society*, 2013, 160, A786-A792.
10. M. Sathiya, G. Rousse, K. Ramesha, C. P. Laisa, H. Vezin, M. T. Sougrati, M. L. Doublet, D. Foix, D. Gonbeau, W. Walker, A. S. Prakash, M. Ben Hassine, L. Dupont and J. M. Tarascon, *Nat Mater*, 2013, 12, 827-835.
11. N. Yabuuchi, R. Hara, M. Kajiyama, K. Kubota, T. Ishigaki, A. Hoshikawa and S. Komaba, *Advanced Energy Materials*, in-press, DOI: 10.1002/aenm.201301453.
12. K. Momma and F. Izumi, *J. Appl. Crystallogr.*, 2008, 41, 653-658.
13. J. M. Paulsen, R. A. Donaberger and J. R. Dahn, *Chemistry of Materials*, 2000, 12, 2257-2267.
14. E. Nishibori, M. Takata, K. Kato, M. Sakata, Y. Kubota, S. Aoyagi, Y. Kuroiwa, M. Yamakata and N. Ikeda, *Nuclear Instruments & Methods in Physics Research Section a-Accelerators Spectrometers Detectors and Associated Equipment*, 2001, 467, 1045-1048.
15. F. Izumi and K. Momma, *Solid State Phenom.*, 2007, 130, 15-20.
16. J. Billaud, G. Singh, A. R. Armstrong, E. Gonzalo, V. Roddatis, M. Armand, T. Rojo and P. G. Bruce, *Energy & Environmental Science*, 2014, 7, 1387-1391.
17. M. Jiang, B. Key, Y. S. Meng and C. P. Grey, *Chemistry of Materials*, 2009, 21, 2733-2745.
18. N. Yabuuchi, K. Yoshii, S.-T. Myung, I. Nakai and S. Komaba, *Journal of the American Chemical Society*, 2011, 133, 4404-4419.
19. Z. Lu and J. R. Dahn, *J. Electrochem. Soc.*, 2001, 148, A1225-A1229.
20. R. Stoyanova, D. Carlier, M. Sendova-Vassileva, M. Yoncheva, E. Zhecheva, D. Nihtianova and C. Delmas, *Journal of Solid State Chemistry*, 2010, 183, 1372-1379.
21. G. Singh, B. Acebedo, M. C. Cabanas, D. Shanmukaraj, M. Armand and T. Rojo, *Electrochemistry Communications*, 2013, 37, 61-63.